AN EQUATION OF MOTION FOR BUBBLE GROWTH

F. J. Lesage°,**, J.S. Cotton°, A.J. Robinson°,*

° McMaster University, Department of Mechanical Engineering, Hamilton, ON, Canada.
**Department of Mathematics, Collège d'Enseignement Général et Professionnel de L'Outaouais, Gatineau, Québec, Canada.
*Trinity College Dublin, Department of Mechanical and Manufacturing Engineering, Dublin 2, Ireland.

ABSTRACT

A mathematical model is developed which describes asymmetric bubble growth, either during boiling or bubble injection from submerged orifices. The model is developed using the integral form of the continuity and momentum equations, resulting in a general expression for the acceleration of the bubble's centre of gravity. The proposed model highlights the need to include acceleration due to an asymmetric gain or loss of mass in order to accurately predict bubble motion. Some scenarios are posed by which the growth of bubbles, particularly idealized bubbles that remain a section of a sphere, must include the fact that bubble growth can be asymmetric. In particular, for approximately hemispherical bubble growth the sum of the forces acting on the bubble is negligible compared with the asymmetric term. Further, for bubble injection from a submerged needle this component in the equation of motion is very significant during the initial rapid growth phase as the bubble issues from the nozzle changing from a near hemisphere to truncated sphere geometry.

INTRODUCTION

Perhaps the oldest and most widely used method for heat transfer enhancement is nucleate boiling. Whether in pool boiling or convective boiling applications, the extremely high heat transfer rates associated with the nucleate pool boiling phenomenon are intimately linked to the vapour bubbles which form, grow and depart at the heated surface. Energy is introduced into the liquid by conduction from the heated solid surface and is stored within a thin thermal boundary layer adjacent to that surface. This stored energy is ultimately used to vaporize the liquid and cause bubbles to form and grow. In addition to evaporative cooling effects, fluid motions induced by bubble activity disrupt the thermal boundary layer in the vicinity of the bubbles causing enhanced mixing and improved heat transfer in these regions [1].

As detailed by Dhir [2], in the past a number of purely empirical and mechanism-based correlations have been developed for predicting nucleate pool boiling heat transfer rates. The empirical approach has resulted in correlations which show different functional dependence on the important boiling parameters. Very often, the predictive capabilities of the empirical correlations fall off rapidly once outside of the range in which the correlations were developed.

Mechanism-based correlations combine information about the underlying sub-phenomena including, but not limited to, bubble waiting time, growth times, heat flux contributions of the microlayer and transient conduction combined with information about the active site density and natural convection to predict the boiling heat transfer rates. A particularly insightful and practical model was put forth by Judd and Hwang [3]. Here, the contributions of transient conduction, microlayer evaporation and natural convection during single bubble events were combined with information about the bubble emission frequency in an attempt to formulate a straightforward and mechanistic model which could predict the wall heat fluxes during boiling.

An alternative approach is the development of accurate numerical simulations of boiling [2]. In fact, the beginning of this century has seen a notable increase in the number of archival publications related to numerical modelling of heterogeneous bubble growth in partial nucleate boiling [4-11] along with many other boiling scenarios such as convective boiling, bubble merger and boiling in mini/micro channels. As the case in question is a highly non-linear, transient multiphysics phenomenon involving the coupled interaction of three phases with extreme gradients, in particular near the triple contact line, the computational expense is very high. As a result, the numerical models must incorporate some simplifying assumptions which largely depend on the aim of the particular investigation. For example, in [4-10], the simulated bubbles were initially unrealistically large compared with that of an actual nucleation cavity so that the vapour temperature remains at the saturation temperature corresponding with the system pressure during the entire growth period. This assumption can be rationalized in these cases since the primary focus was on the bubble dynamics and heat transfer for bubbles growing in the thermally controlled bubble growth domain. Robinson and Judd [2001] developed a model in which bubble growth on a heated surface was initiated from a sub-micron nucleus initially at the wall temperature, which expanded through each of the surface tension, transition and diffusion controlled growth regimes. The numerical simulation was able to resolve bubble growth over several time and length scales due to a hemispherical bubble shape assumption, which allowed the moving interface

to be tracked without skewing of the mesh, as well as the implementation of a 4th order Runga-Kutta scheme. The mathematical modelling of the problem resulted in a set of three coupled differential equations; one for the time rate of change of the vapour temperature, one for the time rate of change of the radius and one for the time rate of change of the interface velocity. Even though this methodology provided the required temporal and spatial resolution for numerically simulating heterogeneous bubble growth over many time and length scales, the equation set is only valid for hemispherical bubbles such as those measured experimentally by Lee and Merte [12] in their microgravity experiments. More realistically, bubbles grow from nearly hemispherical during an initial rapid expansion phase to truncated spherical or oblate spherical segments during a slower upward translation stage, and as near perfect or elongated spheres during the departure stage. In order to utilize a solution technique similar to that of Robinson and Judd [11], a new set of coupled differential equations must be developed to account for the geometric evolution of the bubble from nearly hemispherical, through a truncated spherical segment to spherical at or near departure. In particular, equations which accurately describe the time rate of change of a geometric parameter, such as the position and velocity of the centre of gravity, are required. A similar approach has been used by Li et al. [13] to model bubble growth from a submerged orifice.

In this work a general equation of motion for the centre of gravity of a bubble is derived by considering the upward momentum of a bubble growing in an otherwise quiescent liquid. The equation of motion takes its final form after implementing the integral form of the continuity and momentum equations for the growing gas/vapour bubble. The efficacy of the model is investigated by considering two bubble growth scenarios: hemispherical bubble growth with uniform vaporization and adiabatic bubble growth from a submerged needle orifice. This latter carries forward from a large body of work which deals with bubble growth dynamics and departure which has been reviewed in detail by Kulkarni and Joshi [14]. In our model however, we have alleviated the often used simplifying assumption that the bubble remains a perfect sphere during growth [15]. Here, the bubble remains a portion of a sphere during its growth cycle; in the earliest stage it is a hemisphere which changes to a truncated sphere and evolves to a full sphere near departure. Finally the model is discussed with respect to experimental measurements of bubble growth from a submerged needle for a fixed volumetric flow rate.

MATHEMATICAL MODEL OF BUBBLE GROWTH

Motion of centre of gravity

Figure 1 depicts a bubble of radius R into an otherwise quiescent liquid. In the modelling of this problem the equations are initially left as generic as possible though later it is assumed that the bubble remain a section of a sphere throughout its growth such that the centre of curvature, s, is constant along the entire gas-liquid interface at any instant in time.

By definition, the location of the centre of mass, $\vec{H}$, is given by the expression,

$$m\vec{H} = \int \rho \vec{r} dV \tag{1}$$

where $\vec{r}$ is the position vector within the material volume. Differentiating with respect to time Eq.(1) becomes,

$$\dot{m}\vec{H} + m\dot{\vec{H}} = \frac{d}{dt}\int \rho \vec{r} dV \tag{2}$$

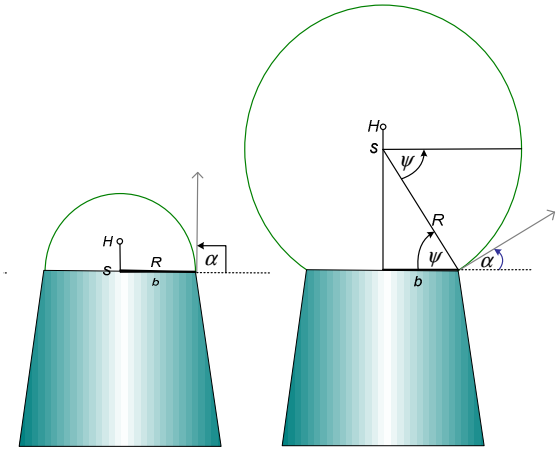

Figure 1b
Ψ and s are both zero

Figure 1c
Ψ and s are positive

Figure 1: Generic bubble growing from an orifice.

Applying Leibniz's theorem, noting that $\vec{r}$ is independent of time and substituting the definition of the total mass within the bubble volume,

$$m = \int \rho dV \tag{3}$$

one obtains,

$$\begin{aligned} m\dot{\vec{H}} &= \int \frac{d}{dt}(\rho\vec{r})dV + \int \vec{n}\cdot\vec{w}(\rho\vec{r})dS - \dot{m}\vec{H} \\ &= \int \vec{r}\frac{d}{dt}(\rho)dV + \int \vec{n}\cdot\vec{w}(\rho\vec{r})dS - \vec{H}\frac{d}{dt}\int \rho dV \end{aligned} \tag{4}$$

The differential form of the continuity equation is,

$$\frac{d}{dt}(\rho) = -div(\rho\vec{v}) \tag{5}$$

Substituting Eq.(5) into Eq.(4) and once again applying Leibniz's theorem, the motion of the centre of mass of the bubble can be described by the expression,

$$\begin{aligned} m\dot{\vec{H}} &= -\int \vec{r}\,div(\rho\vec{v})dV + \int \vec{n}\cdot\vec{w}(\rho\vec{r})dS \\ &\quad - \vec{H}\left[\int \frac{d}{dt}(\rho)dV + \int \vec{n}\cdot\vec{w}\rho dS\right] \end{aligned} \tag{6}$$

One notes that from vector properties the following relation can be utilized,

$$div(\rho\vec{v}\vec{r}) = \vec{r}\,div(\rho\vec{v}) + \rho\vec{v}\cdot\overrightarrow{grad}(\vec{r}) \tag{7}$$

such that,

$$\vec{r}\,div(\rho\vec{v}) = div(\rho\vec{v}\vec{r}) - \rho\vec{v} \tag{8}$$

since for the situation at hand $\overrightarrow{grad}(\vec{r}) = I$ where I is the identity matrix. Substituting Eq.(8) into Eq.(6) yields,

$$\begin{aligned} m\dot{\vec{H}} &= \int \rho\vec{v}dV - \int div(\rho\vec{v}\vec{r})dV + \int \vec{n}\cdot\vec{w}(\rho\vec{r})dS \\ &\quad - \vec{H}\int \frac{d}{dt}(\rho)dV - \vec{H}\int \vec{n}\cdot\vec{w}\rho dS \\ &= \int \rho\vec{v}dV - \int div(\rho\vec{v}\vec{r})dV + \int \rho\vec{n}\cdot\vec{w}\left(\vec{r} - \vec{H}\right)dS \\ &\quad + \vec{H}\int div(\rho\vec{v})dV \end{aligned} \tag{9}$$

where the continuity equation has been substituted and terms grouped. Applying Gauss' Theorem this expression simplifies to,

$$\begin{aligned} m\dot{\vec{H}} &= \int \rho\vec{v}dV - \int \rho\vec{n}\cdot(\vec{v}\vec{r})dS + \int \rho\vec{n}\cdot\vec{w}\left(\vec{r} - \vec{H}\right)dS \\ &\quad + \vec{H}\int \rho\vec{n}\cdot\vec{v}dS \end{aligned} \tag{10}$$

Grouping of terms results in the following equation which describes the motion of the centre of mass of the bubble,

$$m\dot{\vec{H}} = \int \rho\vec{v}dV - \int \rho\vec{n}\cdot(\vec{v} - \vec{w})(\vec{r} - \vec{H})dS \tag{11}$$

The first term on the right hand side (RHS) is the momentum of the vapour bubble and the second term accounts for the fact that the centre of mass of the bubble can move due to an asymmetric gain or loss of mass from the region [16]. The importance of this expression lies in the fact that the product of the instantaneous mass and the velocity of the centre of mass is not necessarily equal to the momentum of the bubble. An example of this would be a quiescent liquid drop on a superheated surface in which evaporation only occurs along the bottom portion of the drop. Since the liquid within the drop has no bulk velocity its momentum is zero. However, if the drop is vaporizing asymmetrically, the centre of gravity will move and this can be described by the asymmetric loss term provided that sufficient information is available to model the vaporization dynamics and drop geometry.

Generalized momentum equation for non-symmetric bubble expansion of variable mass

Differentiating Eq.(11) with respect to time renders the following expression,

$$\begin{aligned} \frac{d(m\dot{\vec{H}})}{dt} = \dot{m}\dot{\vec{H}} + m\ddot{\vec{H}} &= \frac{d}{dt}\int \rho\vec{v}dV \\ &\quad - \frac{d}{dt}\int \rho\vec{n}\cdot(\vec{v} - \vec{w})(\vec{r} - \vec{H})dS \end{aligned} \tag{12}$$

As a result, the acceleration of the centre of mass can be described by,

$$\begin{aligned} m\ddot{\vec{H}} &= -\dot{\vec{H}}\frac{d}{dt}\int \rho dV + \frac{d}{dt}\int \rho\vec{v}dV \\ &\quad - \frac{d}{dt}\int \rho\vec{n}\cdot(\vec{v} - \vec{w})(\vec{r} - \vec{H})dS \end{aligned} \tag{13}$$

The 2nd term on the RHS of Eq.(13) represents the integral form of the momentum equation for the region defined by the bubble which is related to the rate at which momentum crosses the interface due to mass transfer as well as the net force acting on the bubble [16]. The integral form of the momentum equation for an Arbitrary Region (AR) of surface area S is,

$$\frac{d}{dt}\int_{AR(t)} \rho\vec{v}dV = -\int_S \rho\vec{n}\cdot(\vec{v} - \vec{w})\vec{v}dS + \sum \vec{F} \tag{14}$$

where $\sum \vec{F}$ is the sum of the forces acting on that region, which will be discussed in a subsequent section. Substituting Eq. (14) into Eq. (13) yields,

$$\begin{aligned} m\ddot{\vec{H}} &= -\dot{\vec{H}}\frac{d}{dt}\int \rho dV - \int \rho\vec{n}\cdot(\vec{v} - \vec{w})\vec{v}dS \\ &\quad - \frac{d}{dt}\int \rho\vec{n}\cdot(\vec{v} - \vec{w})(\vec{r} - \vec{H})dS + \sum \vec{F} \end{aligned} \tag{15}$$

Applying Leibniz's Theorem followed by the continuity equation results in the expression,

$$\begin{aligned} m\ddot{\vec{H}} &= \dot{\vec{H}}\left[\int div(\rho\vec{v})dV - \int \rho\vec{n}\cdot\vec{w}dS\right] \\ &\quad - \int \rho\vec{n}\cdot(\vec{v} - \vec{w})\vec{v}dS \\ &\quad - \frac{d}{dt}\int \rho\vec{n}\cdot(\vec{v} - \vec{w})(\vec{r} - \vec{H})dS + \sum \vec{F} \end{aligned} \tag{16}$$

Rearranging Eq.(16) and simplifying with the help of Gauss' Theorem yields a general expression for the motion for the centre of mass of a bubble of variable mass which is growing asymmetrically,

$$\begin{aligned} m\ddot{\vec{H}} &= -\int \rho\vec{n}\cdot(\vec{v} - \vec{w})(\vec{v} - \dot{\vec{H}})dS \\ &\quad - \frac{d}{dt}\int \rho\vec{n}\cdot(\vec{v} - \vec{w})(\vec{r} - \vec{H})dS + \sum \vec{F} \end{aligned} \tag{17}$$

Here, the first and last terms on the RHS account for the momentum of the gas/vapour crossing the interface and the sum of the forces acting on the bubble respectively. The second term, however, is typically unaccounted for in previous bubble growth models in that it accounts for the acceleration of the centre of mass due to asymmetry. As will be discussed, there are practical scenarios, in particular those in which the linear momentum is negligible, in which the asymmetry term is in fact dominant.

FORCES ACTING ON GROWING BUBBLE

From this point onward only bubbles that remain a spherical segment during growth will be considered as depicted in Fig. 2. The net force acting on the bubble is the sum of the upward and downward forces acting on the bubble

boundary and the force acting on the contact line at the triple interface [17].

The downward forces acting on the bubble are the drag force, F_d and the capillary or surface tension force, F_c. Without resorting to solving the fully viscous governing equations for the flow around the bubble an approximate approach is typically used to calculate the influence of the drag force. For a needle injected bubble the drag force can be approximated as [18],

$$F_d = \frac{1}{2}\rho_l C_D \pi s^2 \dot{s}^2 \tag{18}$$

where C_D is the drag coefficient for a spherical bubble issuing from a submerged needle which can be approximated as [18],

$$C_D = \frac{24}{\mathrm{Re}}\left(1+\frac{3}{8}\mathrm{Re}\right), \quad \mathrm{Re} = \frac{\rho_l \dot{H} D}{\mu} \tag{19}$$

The drag force is generally quite small and often inviscid liquids are assumed in the theoretical modelling [17]. For situations in which the bubble is expanding rapidly with small degrees of truncation, the efficacy of this type of empirical approach is uncertain.

The capillary force occurs at the contact line of the three intersecting surfaces: solid, liquid and gas/vapour. Integrating about this line yields the capillary force,

$$\vec{F}_c = -2\int_0^{\pi} b\sigma\vec{t}(\varphi)d\varphi \tag{20}$$

in which $\vec{t}$ is a unit vector tangent to the interface of the bubble and normal to the contact line and the negative sign represents the inward direction of the force. Geometrically the above implies that for some angle φ,

$$t_{xy} = \|\vec{t}\|\cos\alpha$$
$$t_z = \|\vec{t}\|\sin\alpha$$

in which $t_{xy} = t_x\vec{e}_x + t_y\vec{e}_y$. The components of $\vec{t}$ are thus,

$$t_x = \|\vec{t}\|\cos\alpha\cos\varphi$$
$$t_y = \|\vec{t}\|\cos\alpha\sin\varphi$$
$$t_z = \|\vec{t}\|\sin\alpha$$

The above shows that when integrating over the contact line, the *x* component and the *y* component cancel each other out as would be expected with such spherical symmetry about the *z* axis. Furthermore, the *z* component is independent of φ. That is, the *z* component of the capillary force is the same at all points along the contact line which is, once again, as to be expected with the spherical symmetry of the problem. Thus the capillary force becomes,

$$F_c = 2\int_0^{\pi} b\sigma\|\vec{t}\|\sin\alpha d\varphi = 2\pi b\sigma\|\vec{t}\|\sin\alpha = 2\pi\sigma\|\vec{t}\|\frac{b^2}{R} \tag{21}$$

In Duhar and Colin [15] and Klausner et al. [19] the above vector $\vec{t}$ is a unit vector and thus the capillary force for an axisymmetric bubble becomes,

$$F_c = -\frac{2\pi\sigma b^2}{R} \tag{22}$$

The buoyancy force is obtained by integrating the hydrostatic component of the liquid pressure over the bubble cap only,

$$F_b = \int(\rho_l - \rho_g)g dV \tag{23}$$

For a spherical segment this involves only the volume of the region with liquid both above and below the section of the bubble cap such that,

$$F_b = (\rho_l - \rho_g)g\left(\frac{4\pi s^3}{3}\right) \tag{24}$$

In this way, the bouyancy force correctly approaches zero for a hemispherical bubble.

The force due to contact pressure is obtained by integrating along the bubble base and is sometimes referred to as a bouyancy correction force,

$$\vec{F}_p = \int \vec{n}\cdot(-pI)dS \tag{25}$$

Due to the axisymmetry of the bubble, only the *z* direction is considered yielding a contact pressure of,

$$F_p = \int(n_z p)dS = \pi(p_g - p_l)b^2 \tag{26}$$

Applying the Young-Laplace equation at the bubble interface the gas and liquid pressures are related through the expression,

$$p_g - p_l = \frac{2\sigma}{R} \tag{27}$$

where it is understood that the local liquid pressure acting on the interface is the sum of the static and dynamic pressures. Substituting into Eq.(26) gives,

$$F_p = \frac{2\pi\sigma b^2}{R} \tag{28}$$

It is noted that for a bubble that retains the shape of a spherical segment, the contact pressure force and the capillary force are equal yet opposite and thus have exactly offsetting effects on the growth of the bubble.

Finally, for a bubble growing due to gas injection the momentum of the injected gas must be considered [18]. For vapour bubbles growing due to vaporization of the liquid into the bubble a similar momentum force does not effect the behavior and should not appear in the equation of motion [18]. For gas injected bubbles the conservation of mass principal applies and for a constant volumetric flow rate of gas being injected into the bubble that passes through the foot of the bubble with fixed radius *b*, the following holds*;*

$$\dot{V}_{needle} = \pi b^2 v_g \tag{29}$$

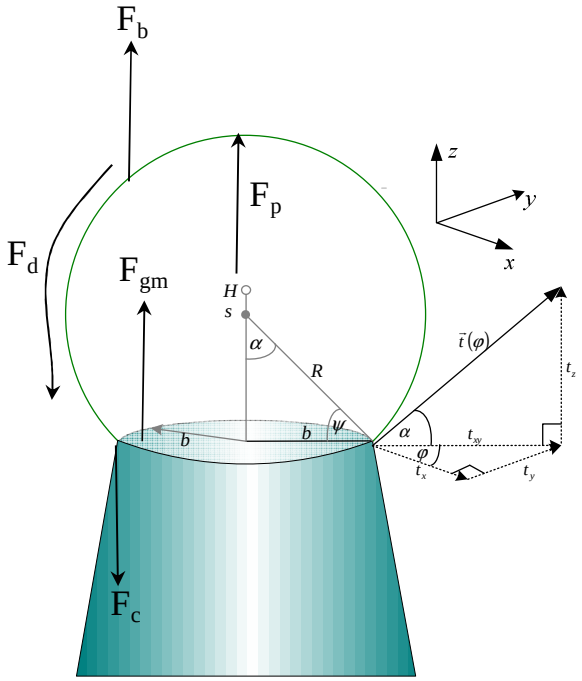

Figure 2: Geometric parameters for a truncated bubble growing from and orifice.

The equivalent force due to the gas momentum entering the bubble is thus,

$$F_{gm} = \dot{m} v_g = \rho_g \dot{V}_{needle} v_g \tag{30}$$

Substituting into the above yields,

$$F_{gm} = \frac{\rho_g}{\pi b^2} \dot{V}^2_{needle} \tag{31}$$

As with the drag force, this force is very often negligibly small compared with the buoyancy, surface tension and contact pressure forces during the later stages of growth such as that occurring near bubble departure.

Finally, the sum of the vertical forces acting on the bubble which influence its upward momentum is approximately,

$$\sum F = \underbrace{F_d + F_c}_{\substack{\text{downward} \\ \text{forces}}} + \underbrace{F_p + F_b + F_{gm}}_{\substack{\text{upward} \\ \text{forces}}} \tag{32}$$

where it is understood that upward forces are positive and downward forces are taken as negative.

HEMISPHERICAL BUBBLE GROWTH WITH UNIFORM VAPORIZATION

At this juncture it is instructive to consider a rather extreme yet realistic scenario to exemplify the significance of the modelling approach proposed in this study. Consider the case of a bubble growing in microgravity initiating from a small nucleation site on a superheated surface. Bubble growth is initiated at the end of the waiting time and the bubble is growing as a near perfect hemisphere as is the case with the space microgravity experiments of Lee and Merte [12]. In this particular scenario, Robinson [20] showed that during the early growth stages the thermal boundary layer adjacent to the heated surface is very large compared with the size of the bubble so that the superheat around the bubble dome is nearly constant and vaporization can be approximated as uniform over the bubble surface. If this is approximately the case then $-\rho \vec{n} \cdot (\vec{v} - \vec{w}) = \dot{m} / A$ and, combined with the fact that $s = 0$ for a hemispherical bubble, the equation of motion for the centre of gravity simplifies to,

$$m\ddot{H} = \dot{m}(v_z - \dot{H}) + \frac{1}{8}\frac{d}{dt}[\dot{m}R] + \sum F \tag{33}$$

However, in this scenario the buoyancy force is zero due to the absence of gravity. In a gravitational field, provided the bubble is hemispherical, this would also be true since $F_b = 0$ for $s = 0$ as given in Eq. 24. Due to the geometry of the bubble the contact pressure force and the capillary force are equal and offsetting which, for this idealized scenario, causes the sum of the forces to be exactly equal to zero. This is provided that the drag force can be considered very small, which in this case is rational since the expansion is almost radially symmetric so that the liquid flow is nearly irrotational. The main result here is that the linear momentum of the bubble is zero, in that it is not a force imbalance that causes the centre of gravity to accelerate. In this scenario the motion of the centre of gravity is solely described by geometric and mass transfer factors opposed to mechanistic influences. From the above assumption that the vaporization is uniform, and the linear momentum and force summation are both zero, one obtains the expression

$$m\ddot{H} = -\dot{m}\dot{H} + \frac{1}{8}\frac{d}{dt}[\dot{m}R] \tag{34}$$

Furthermore, the geometric simplification results in a relation between the centre of gravity and the bubble radius such that,

$$H = s + \frac{3(R-s)^2}{4(2R-s)} = \frac{3}{8}R \tag{35}$$

As a result, the governing equation for hemispherical bubble growth in terms of the radius is,

$$m\ddot{R} = -\frac{2}{3}\dot{m}\dot{R} + \frac{1}{3}\ddot{m}R \tag{36}$$

The correctness of Eq.(36) is easily shown by substituting $m = \rho_v (2/3)\pi R^3$ in the above expression and differentiating for a constant vapour density.

BUBBLE GROWTH FROM A SUBMERGED NEEDLE

A simple experiment was performed in which an air bubble was injected into an otherwise quiescent pool of water at room temperature. The air volumetric flow rate was regulated by a controllable syringe pump and kept constant at 0.95 mm^3/ms and the bubble growth was recorded using a high-speed camera operating at 1000 frames/second. A sample of the recorded images is shown in Fig.3. It is evident that after a period of time a nearly hemispherical bubble issues from the

needle with a base diameter approximately that of the needle inner radius, which in this investigation was 0.42 mm. For the first several milliseconds the bubble retains a shape which is very close to a spherical segment. Beyond approximately 5 ms a small neck begins to form so that the spherical segment shape assumption becomes progressively less realistic.

Figure 4 shows the time evolution of the radius, R, the centre of curvature, s, and the ratio s/R for the entire bubble growth cycle. The important feature here is that there is an early phase of rapid expansion in which s/R increases from 0 quickly approaching unity as the bubble becomes almost spherical (i.e. s/R~1). In this initial growth regime the influence of the asymmetric gain term in Eq.(17) is expected to be significant.

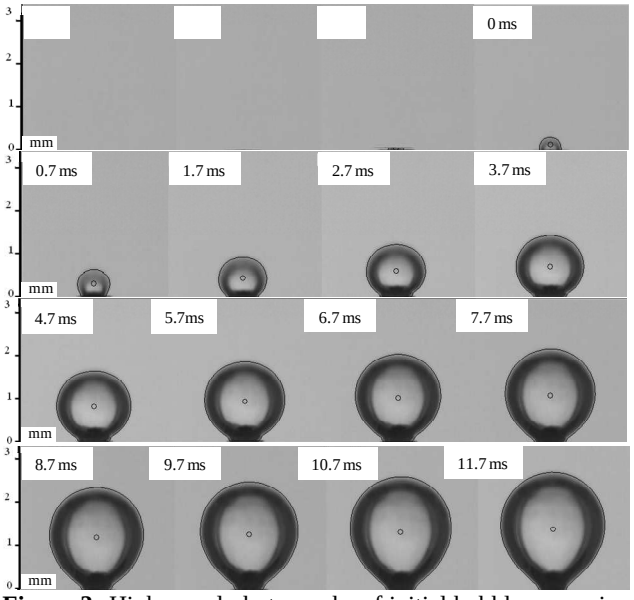

Figure 3: High speed photographs of initial bubble expansion from a submerged orifice for a constant volumetric flow rate of 0.95 mm/ms

Again it will be assumed here that the linear momentum of the gas bubble is negligibly small so that the bubble evolves in a quasi-equilibrium manner such that,

$$m\dot{H} = -\int_A \rho(v_z - w)(r_z - H)dS \tag{37}$$

where

$$\frac{\dot{m}}{A} = -\rho(v_z - w) \tag{38}$$

is constant and A is the base bubble area. This results in the simplification,

$$\begin{aligned} \dot{H} &= \frac{\dot{V}}{AV}\int_A (r_z - H)dS \\ &= \frac{\dot{V}}{2\pi b^2 V}\left(\pi R(R+s)^2 - 2\pi HR(R+s)\right) \end{aligned} \tag{39}$$

Utilizing the appropriate geometric relations Eq.(39) can be expressed in terms of R and integrated and rearranged for the time, t, it takes to achieve a given radius,

$$t = \frac{\pi b^2}{3\dot{V}}\left[\frac{4R^3}{3b^2} + 5R + s\left(\frac{4R^2}{3b^2} + \frac{17}{3}\right) - \frac{19}{3}b\right] \tag{40}$$

where $s = (R^2 - b^2)^{1/2}$. The results are plotted in Fig. 5 along with the experimental data. Clearly there is very good agreement in the early growth as the bubble tends to grow as a spherical segment in this region. Beyond approximately 5 ms the agreement becomes progressively worse as the bubble tends to lose its spherical shape and elongate as the neck forms.

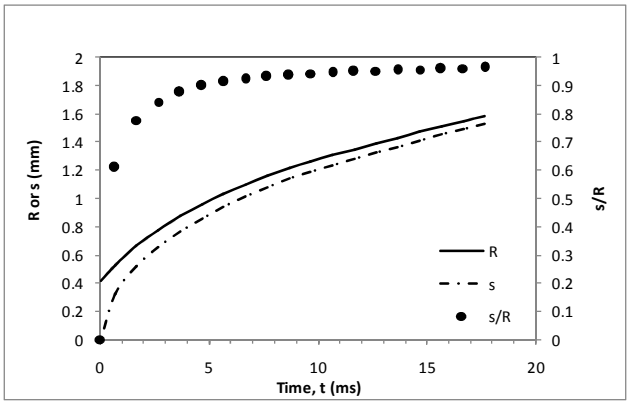

Figure 4: Growth histories of R, s and s/R corresponding with the measurements in Figure 3.

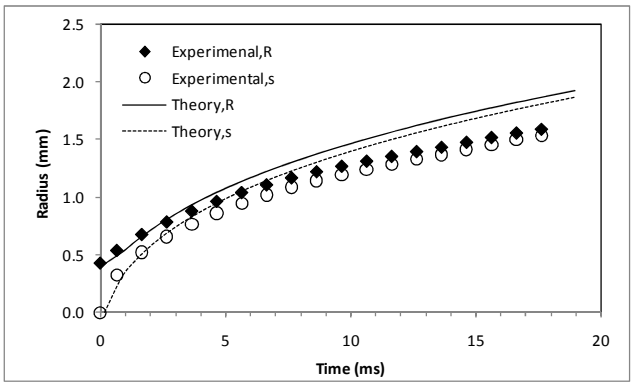

Figure 5: Experimental and predicted growth curves

CONCLUSION

A mathematical model is presented for bubble expansion beginning from the definition of the gas/vapour momentum. Combining this analysis with the integral form of the momentum and continuity equations results in a generalized equation for the motion of the centre of mass of the bubble of variable mass. Compared with other theories this model takes into account the fact that the centre of gravity can accelerate due to asymmetric gain or loss of mass, which is novel since many earlier models simply equate the bubble momentum to the sum of the forces without considering this effect. The latter assumption is often justifiable in late stage growth. However, it has been shown that there are cases, such as the initial rapid expansion from a submerged needle and boiling on a heated surface with a moving contact line where the asymmetry of the bubble requires that this term be included in describing its motion.

ACKNOWLEDGEMENTS

We gratefully acknowledge the support from Science Foundation Ireland (SFI) through grant number RFP/ENMF 249 as well as Abdulaleem Albadawi and Paul Rosemond for their assistance.

NOMENCLATURE

s	Centre of curvature
H	Centre of mass (z component)
R	Bubble radius
b	Needle tip radius is constant
$\vec{v}$	Fluid velocity
$\vec{w}$	Surface velocity
φ	Temporal limit angle
α	Contact angle
g	Gravitational constant
ρ_g, ρ_v	Density of injected gas/vapour
ρ_l	Density of liquid
P_l	Pressure of liquid
P_g, P_v	Pressure of gas/vapour
m	Mass within the bubble
μ	Viscosity
σ	Surface tension
Re	Reynold's number
$\dot{V}_{needle}$	Volumetric flow rate of injected gas.
C_D	Drag coefficient
F_d	Drag force
F_c	Capillary force
F_b	Buoancy force
F_p	Force due to contact pressure
F_{gm}	Force due to gas momentum

REFERENCES

1. V.K. Dhir, Nucleate and transition boiling heat transfer under pool and external flow conditions, *Int. J. Heat and Fluid Flow*, vol. 12 no.4, pp. 290-314, 1991.
2. V.*K.* Dhir, Mechanistic Prediction of Nucleate Boiling Heat Transfer–Achievable or a Hopeless Task?, *J. Heat Trans.*, vol. 128, p.1-12, 2006.
3. R.L. Judd and K.S. Hwang, A comprehensive model for nucleate pool boiling heat transfer including microlayer evaporation, *J. Heat Trans*, vol. 98, pp. 623-629, 1976.
4. Q. Bai and Y. Fujita, Numerical simulation of bubble growth in nucleate boiling - Effects of system parameter, *Multiphase Sci. Tech.*, vol. 12 no. 3-4, pp. 195-214, 2000.
5. H.Y. Yoon, S. Koshizuka and Y. Oka, Direct calculation of bubble growth, departure, and rise in nucleate pool boiling, *Int. J. Multiphase Flow*, vol. 27, pp.277-298, 2001.
6. P. Genske and K. Stephan, Numerical simulation of heat transfer during growth of single vapor bubbles in nucleate boiling, *Int. J. Thermal Sci.*, vol. 45 no.3, pp. 299-309, 2006.
7. T. Fuchs, J. Kern and P. Stephan, A transient nucleate boiling model including microscale effects and wall heat transfer, *J. Heat Transfer*, vol. 128 no.12, pp.1257-1265, 2006.
8. J. Wu, V.K. Dhir and J. Qian, Numerical simulation of subcooled nucleate boiling by coupling level-set method with moving-mesh method, *Numerical Heat Transfer, Part B: Fundamentals*, vol. 51 no.6, pp. 535-563, 2007.
9. P. Stephan and T. Fuchs, Local heat flow and temperature fluctuations in wall and fluid in nucleate boiling systems, *Heat Mass Transfer*, DOI:10.1007/s00231-007-0320-1 (2007).
10. A. Mukherjee and S.G. Kandlikar, Numerical study of single bubbles with dynamic contact angle during nucleate pool boiling, *Int. J. Heat Mass Trans.*, vol. 50 no.1-2, pp.127-138, 2007.
11. A.J. Robinson and R.L. Judd, Bubble growth in a uniform and spatially distributed temperature field, *Int. J. Heat Mass Transfer*, vol. 44, pp.2699-2710, 2001.
12. H.S. Lee and H. Merte Jr., Hemispherical bubble growth in microgravity: experiments and model, *Int. J. Heat Mass Transfer*, vol. 39, pp.2449-2461, 1996.
13. H.Z. Li, Y. Mouline and N. Midoux, Modelling the bubble formation dynamics in non-Newtonian fluids, *Chem. Eng. Sci*., vol. 57 no. 3, pp. 339-346, 2002.
14. A.A. Kulkarni and J.B. Joshi, Bubble formation and bubble rise velocity in gas-liquid systems: A review, *Ind. Eng. Chem. Research*, vol. 44 no.16, pp. 5873-5931, 2005.
15. G. Duhar and C. Colin, Dynamics of bubble growth and detachment in a viscous shear flow, *Phys. Fluids*, vol. 18, art. no. 077101 (2006).
16. R.L. Panton, Incompressible flow, Wiley, New York, N.Y., 1984.
17. Y.A. Buyevich and B.W. Webbon, Bubble formation at a submerged orifice in reduced gravity, *Chem. Eng. Sci.*, vol. 51 no.21, pp. 4843-4857, 1996.
18. S.K. Kasimsetty, A. Subramani, R.M. Manglik and M.A. Jog, Theoretical modelling and experimental measurements of single bubble dynamics from a submerged orifice in a liquid pool, *Proc. ASME-JSME Thermal Engineering Summer Heat Transfer Conference*, HT2007-32088, July, 2007.
19. J.F. Klausner, R. Mei, M.D. Hernhard and L. Z. Zeng, Vapour bubble departure in forced convection boiling, *Int. J. Heat Mass Transfer*, vol. 36, pp.651-662, 1993.
20. A.J. Robinson, Bubble growth dynamics in uniform and non-uniform temperature fields, Ph.D. Thesis, McMaster University, Hamilton, Ontario, Canada, (2002).
21 W.G.J. Van Helden, C.W.M. Van Der Geld and P.G.M. Boot, Forces on bubbles growing and detaching in flow along a vertical wall, *Int. J. Heat Mass Transfer*,vol. 38 no. 11, pp. 2075'2088, 1995.